Spectral diffusion, phonon echoes, and saturation recovery in glasses at low temperatures

J. L. Black*†

Division of Engineering and Applied Physics, Harvard University, Cambridge, Massachusetts 02138

B. I. Halperin*

Department of Physics, Harvard University, Cambridge, Massachusetts 02138

(Received 6 May 1977)

Many features of glasses below 1 K are explicable in terms of localized tunneling levels, for which a spin-$\frac{1}{2}$ analogy exists. Here we show that spectral diffusion, resulting from fluctuations in resonant frequency, is essential to our understanding of recent ultrasonic experiments. Our model involves a coupling among the levels of the form $J_{ij}S_z^i S_z^j$, which acquires a time dependence when a spin-flipping rate T_1^{-1} is introduced. For two- and three-pulse phonon-echo experiments near $T = 20$ mK, we predict phase-memory times which agree qualitatively with the experimental results of Golding and Graebner. For saturation recovery, we predict a linewidth whose time dependence should be observable near $T = 100$ mK. Estimates of tunneling-model parameters and comparison with specific-heat experiments suggest that glasses may contain two types of tunneling levels.

I. INTRODUCTION

A. General features of glasses at low temperatures

For some time it has been known that glasses in general exhibit anomalous behavior at low temperatures $(T < 1$ K).[1-4] The specific heat contains a large term which is roughly proportional to T, and the thermal conductivity, varying as T^2, is very small compared to that of crystalline dielectrics. Direct measurements of phonon mean free paths dramatically demonstrate that nonlinear effects (saturation) occur except at very low ultrasonic power levels.[4-6] A variety of other phenomena including anomalous sound velocity,[7,8] anomalous dielectric response,[9] and cross saturation between microwave fields and ultrasonic pulses[10] have also been observed. Most remarkable of all, however, has been the recent discovery of phonon echoes by Golding and Graebner.[11]

All of the properties discussed so far can be understood by assuming that the glassy state includes localized low-lying excitations, which have a roughly constant density of states of order 10^{20} eV^{-1}cm^{-3}. It is sufficient to assume that these excitations are two-level systems, and as such they may be treated as pseudospins. Since the potential energy of a "spin" depends on its atomic environment, each spin is coupled to the local strain field. This coupling not only causes phonon scattering, but it also leads to a strain-mediated coupling among the spins. It has recently been suggested by Joffrin and Levelut[12] and by Hunklinger and Arnold[4] that certain aspects of nonlinear ultrasonic propagation can be understood only by taking into account these "spin-spin" interactions. We have adopted this point of view, paying particular attention to the *time-dependent* shifts in a spin's resonant frequency. Such shifts arise through spin-spin interactions whenever neighboring spins undergo thermal flips. We have treated this phenomenon in glasses within the framework of spectral diffusion as developed by Klauder and Anderson for electron spin resonance.[13] Using this formulation we are able to make predictions for the loss of phase coherence in phonon-echo experiments. We also predict some new time-dependent phenomena which should be observable in ultrasonic saturation experiments.

B. Are there two types of excitations?

An additional objective of this paper is to probe the nature of these hypothetical spins by placing restrictions upon the models which describe them. For this purpose we treat the spins within the framework of the tunneling model, in which we envision groups of atoms tunneling between local minima in the potential energy.

In the usual formulation of this model,[14-17] a distribution of spin-lattice relaxation times is assumed for each tunneling level energy splitting. Long relaxation times correspond to levels which are weakly coupled to phonons. These weakly coupled levels have little direct effect on the ultrasonic properties, which include attenuation, saturation, and phonon echoes. On the other hand, some of these weakly coupled levels contribute to the specific heat, depending on the time scale of the specific-heat experiment. Thus one of the key issues in the tunneling model is understanding the relationship between the strongly coupled excitations, which determine the ultrasonic properties, and the totality of excitations contributing to the specific heat.

The simplest approach to this problem is to assume that all of the localized excitations are of a "standard" type as discussed in Sec. II. These "standard" levels have identical phonon coupling constants γ and belong to a single smooth distribution of barrier heights. The ultrasonic experiments to be discussed in this paper allow us to estimate $\bar{P}$, the density of *strongly coupled* "standard" tunneling levels per unit energy and volume [cf. Eq. (8)]. We are also able to estimate the spin-phonon coupling constant γ, which allows us to compute the relaxation times using Eq. (9).

As is shown in Sec. II, the value of $\bar{P}$ is too small to be consistent with the specific-heat density of states n_0, which is observed[18,19] on a long-time scale (5 sec). Furthermore a specific-heat experiment performed[20] on a short-time scale (<50 μsec) shows little difference from the long-time-scale experiments. This observation may also be inconsistent with an assumption that *all* of the levels are of the standard type. On the other hand, the standard levels do yield quite reasonable frequency and temperature dependences for the phonon mean free path [cf. Eq. (8)].

Since the only difficulties arise when we attempt to deduce n_0 for the specific heat directly from $\bar{P}$, we are led to adopt the following point of view. All ultrasonic properties (e.g., all results in Secs. II–VI) are attributed to interactions between phonons and standard tunneling levels. The specific-heat density of states n_0, however, has contributions from both the standard tunneling levels and additional excitations which we call "anomalous" tunneling levels. Experimental justification for this approach comes from the fact that sample-dependent variations in the specific heat are usually not accompanied by variations in the phonon mean free path.[18,19] Thus the spin-phonon coupling of the anomalous levels must be weaker than that of the standard levels. On the other hand, the anomalous levels must be sufficiently strongly coupled so as to have relaxation times which are shorter than the duration of the heat-pulse experiments.[20] We shall see in Sec. II that there remain difficulties in choosing anomalous-level parameters so as to satisfy both of these conditions.

Having introduced anomalous levels to help explain specific-heat results, we will focus our attention on the standard levels throughout the remainder of this paper. We do this because we are primarily interested in the effect of spin-spin interactions upon ultrasonic properties. Nevertheless our concentration on standard levels will be useful in discussing the more general question of anomalous levels and specific heat. In particular our approach yields estimates of $\bar{P}$ and γ for the standard levels, thereby determining the standard-level contribution to the specific heat on various time scales. The anomalous levels then account for the difference between the standard-level contribution and the experimentally observed value of the specific heat.

II. TUNNELING MODEL

A. Definition of the model

As mentioned above, most of the low-temperature properties of glasses can be explained in terms of localized two-level excitations of unknown origin.[4,14-17] For such excitations there exists a complete analogy[4,5,12] with a collection of $S = \frac{1}{2}$ "spins" in a "static magnetic field" E^i, whose magnitude varies over a wide range ($h^{-1}E_{max} \gtrsim 20$ GHz) from site to site. We thus have a contribution to the Hamiltonian

$$\mathcal{H}_0 = \sum_i E^i S_z^i. \qquad (1)$$

Note that S_z^i has eigenvalues $\pm\frac{1}{2}$ and that E^i is the energy splitting at site i. The conventions used for S_x, S_y, and S_z are shown in Eq. (A1'). It is well established that the two-level excitations are coupled to strain fields and to electric fields, yielding a "spin-magnetic field" interaction of the schematic form (suppressing vector and tensor indices):

$$\mathcal{H}_1 = -\sum_i (B^i \epsilon^i S_x^i + D^i \epsilon^i S_z^i + \bar{\mu}^i F^i S_x^i + \mu^i F^i S_z^i). \qquad (2)$$

In this expression ϵ^i is the strain field at site i, B^i is the off-diagonal elastic-coupling tensor, and D^i is the diagonal elastic-coupling tensor. Correspondingly F^i is the electric field at site i, $\bar{\mu}^i$ is the off-diagonal dipole moment, and μ^i is the diagonal dipole moment. The off-diagonal couplings are responsible for radiation-induced resonant transitions, while the diagonal couplings are responsible for shifts in the effective static magnetic field. The remainder of this paper will be restricted to strain couplings, which are more intrinsic (less sample dependent) than the electric field couplings.[9] It is worth noting, however, that the two coupling mechanisms may be considered as parallel contributors to spin-spin interactions (cf. Sec. III).

The tunneling model is an appealing way to envision the two-level excitations which we have been discussing. The use of this model has the additional advantage of prescribing the relationship between the diagonal coupling D^i and the off-diagonal coupling B^i. The most reliable low-temperature measurements of phonon attenuation[4,21] give information only about B^i, yet we will also

need to know D^i in order to discuss spin-spin interactions in Sec. III.

The physical content of the tunneling model is that certain atoms or groups of atoms of mass m may tunnel between roughly equivalent potential energy minima separated in energy by an asymmetry splitting Δ. The tunneling coupling energy is given by $\Delta_0 = \hbar \tilde{\omega}_0 e^{-\lambda}$, where $\hbar \tilde{\omega}_0$ is a typical zero-point energy in the wells and $\lambda = \hbar^{-1} d (2mV)^{1/2}$ is a parameter describing the extent of wave-function overlap between the states in the wells. Figure 1 shows the prototype configuration with barrier height V and well separation d.

Before diagonalization, the Hamiltonian for each tunneling level (unperturbed by external fields) has the form[14-16]

$$\mathcal{H}_0' = \frac{1}{2}\begin{pmatrix} \Delta & \Delta_0 \\ \Delta_0 & -\Delta \end{pmatrix}, \qquad (3)$$

where, for simplicity, we have suppressed the site index i. The dominant term in the spin-phonon coupling is given by[14-17] (suppressing tensor indices; see Appendix.)

$$\mathcal{H}_1' = -\epsilon \gamma \begin{pmatrix} 1 & 0 \\ 0 & -1 \end{pmatrix}, \qquad (4)$$

where γ is a deformation-potential tensor with a rough magnitude of 1 eV. After diagonalization, Eq. (3) assumes the form of one term in Eq. (1) with $E^i = (\Delta^2 + \Delta_0^2)^{1/2}$. Under the same diagonalizing transformation, Eq. (4) generates both the diagonal and the off-diagonal interactions in Eq. (2). The coupling tensors are related to γ unambiguously by

$$B = 2(\Delta_0/E)\gamma, \quad D = 2(\Delta/E)\gamma. \qquad (5)$$

Detailed predictions of the tunneling model depend upon assumptions made about the distribution of quantities such as Δ, λ, and γ over the ensemble of spins in the sample.[17] A reasonably general prescription is to assume that the distribution function is a slowly varying function of Δ, for Δ in the range of interest (10 mK $< \Delta/k_B <$ 1 K). Then

$$P(\Delta,\lambda)d\Delta d\lambda \approx P(0,\lambda)d\Delta d\lambda \equiv \overline{P}(\lambda)d\Delta d\lambda \qquad (6)$$

is the number of spins per volume with asymmetry Δ and tunneling parameter λ. The excitations described by $\overline{P}(\lambda)$ will be called "standard" tunneling levels. The coupling constant γ is assumed to have a single value for all such spins. The form of $\overline{P}(\lambda)$ is not known *a priori*, but the generic behavior for a continuous distribution of barrier heights is shown in Fig. 2. For a given energy splitting E, the parameter λ must exceed a minimum value $\lambda_{\min}(E) = \ln(\hbar\tilde{\omega}_0/E)$, which corresponds to the maximum value of $B(= 2\gamma)$ and the minimum value of $D(= 0)$ according to Eqs. (5). The characteristics of the spins with energy splitting E vary continuously as λ varies between $\lambda_{\min}(E)$ and some cutoff value $\lambda_{\max}$. This variation leads to the definition of a parameter η which describes the width of $\overline{P}(\lambda)$ with the energy fixed at E:

$$\eta(E) \equiv \lambda_{\max} - \lambda_{\min}(E) + \ln 2. \qquad (7)$$

For the purpose of describing ultrasonic properties it is sufficient to assume that $\overline{P}(\lambda) = \overline{P}$ in the range $\lambda_{\min} < \lambda < \lambda_{\max}$. Thus we can conveniently specify the distribution of standard tunneling levels by the parameter set $(\overline{P}, \gamma, \eta)$.

B. Phonon scattering, relaxation, and specific heat

With the above assumptions, the standard tunneling level contribution to the phonon mean free path due to resonant phonon absorption and emission is given by[14,16]

$$l_\alpha^{-1} = (\pi\omega/\rho c_\alpha^3)\overline{P}\gamma_\alpha^2 \tanh(\hbar\omega/2k_B T), \qquad (8)$$

where $\alpha = l, t$ designates longitudinal or transverse phonon polarization. In Eq. (8), c_α is the appropri-

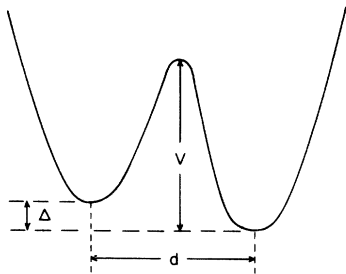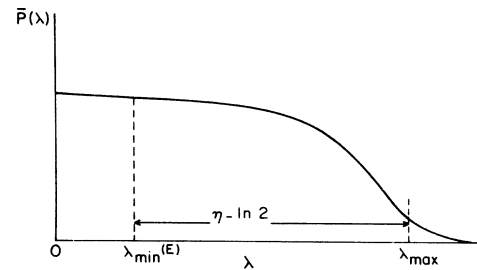
FIG. 1. Tunneling-level potential-energy curve. Parameters shown are asymmetry energy Δ, barrier energy V, and well separation d.

FIG. 2. Sketch of the distribution function $\overline{P}(\lambda)$, which has dimensions (energy)$^{-1}$ (length)$^{-3}$. The parameter η defines the width of the distribution between $\lambda_{\max}$ and the cutoff $\lambda_{\min}(E) = \ln(\hbar\tilde{\omega}_0/E)$.

ate sound velocity, ρ is the mass density of the glass, and ω is the phonon frequency. Direct measurements of longitudinal and transverse ultrasonic attenuation[4,21] are in good agreement with the form of Eq. (8) and determine the products $\bar{P}\gamma_\alpha^2$, thereby reducing the parameter set to (γ_α, η) or $(\bar{P}, \eta)$.

Phonon emission and absorption processes also lead to spin-lattice relaxation for the standard levels. The rate of such relaxation is given by the expression[5,14,16]

$$T_1^{-1}(E,\lambda) = \left(\frac{\gamma_l^2}{c_l^5} + 2\frac{\gamma_t^2}{c_t^5}\right)\frac{E^3 e^{-2(\lambda - \lambda_{min})}}{2\pi\hbar^4\rho} \coth\frac{E}{2k_B T} . \quad (9)$$

From this result it is easy to see that for reasonably large values of η (e.g., $\eta > 5$), the relaxation times vary over several orders of magnitude between the fastest levels ($\lambda = \lambda_{min}$) and the slowest levels ($\lambda = \lambda_{max}$). These relaxation times play a crucial role in determining C_s, the specific heat of the standard tunneling levels[14-16]:

$$C_s = \tfrac{1}{6}\pi^2 k_B^2 n_s T . \quad (10a)$$

Here k_B is Boltzmann's constant and n_s is the (roughly constant) density of states for the standard levels whose spin-lattice relaxation times are shorter than the experimental duration t. The expression for n_s is calculated to be approximately[14,17]

$$n_s = \bar{P}\min[\eta, \tfrac{1}{2}\ln(4R_{max}t)] , \quad (10b)$$

where $R_{max} \equiv T_1^{-1}(E \approx 2k_B T, \lambda = \lambda_{min})$ is the maximum spin-lattice relaxation rate for levels with $E \approx 2k_B T$.

We can now proceed to derive estimates for n_s for various values of t. Recent pulse area measurements done in conjunction with phonon-echo experiments[11] (see Sec. V) have yielded $\gamma_l = 1.6$ eV. By employing the value of $\bar{P}\gamma_l^2$ obtained[21] from ultrasonic attenuation experiments at $\omega/2\pi = 0.5$ GHz, $\bar{P}$ is estimated to be 2.2×10^{31} erg^{-1}cm^{-3} for Suprasil W. Specific-heat measurements[22] on the same material yield values for the observed density of states n_0, ranging from 3.0×10^{32} erg^{-1}cm^{-3} at $E/2k_B = 25$ mK to 9.0×10^{32} erg^{-1}cm^{-3} at $E/2k_B = 1$ K. From Eq. (10b) we can see that the factor multiplying $\bar{P}$ would have to lie roughly between 15 and 40 if we were to demand that n_s equal n_0. This turns out to be impossible for the following reason. Using the estimates[11,21] $\gamma_l = 1.6$ eV and $\gamma_t^2 \approx \tfrac{1}{2}\gamma_l^2$, R_{max} is found to be $1.26 \times 10^3 T^3 \mu$sec^{-1}. Consequently $\tfrac{1}{2}\ln 4R_{max}t$ ranges from 6.4 at $E/2k_B = 25$ mK to 12.0 at $E/2k_B = 1$ K for an experimental time of 5 sec. Thus we see that n_s alone cannot account for the density of states seen in long-time (5 sec) specific-heat experiments.

Even if we could adjust $\bar{P}$ to bring n_s into agree-ment with n_0, we would still run into problems with the heat pulse experiment of Goubau and Tait.[20] For example, at $T = 160$ mK, $\tfrac{1}{2}\ln 4R_{max}t$ changes from 9.2 to 1.5 as the experimental time scale is reduced from 5 sec to 1 μsec (the time required for the heat pulse to cross the sample in the absence of tunneling levels). This change corresponds to an 84% reduction in the specific heat, but such a reduction is not observed in the experiment.[20]

C. "Anomalous" tunneling levels

Difficulties of the type discussed in Sec. II B suggest that standard tunneling levels alone may not be able to explain the specific heat observed in glasses. Consequently we are suggesting the possibility that "anomalous" tunneling levels may exist. These levels may be thought of as a second set of tunneling levels with a density of states n_a and coupling strengths $B_a = 2(\Delta_0^a/E)\gamma_a$ and $D_a = 2(\Delta^a/E)\gamma_a$. Phonon-scattering rates and relaxation times are given by the analogs of Eqs. (8) and (9), respectively. In order that the anomalous levels not contribute significantly to the observed phonon scattering rate, the condition $n_a[(\Delta_0^a/E)\gamma_a]^2 < \bar{P}\gamma^2$ must hold. To have no effect on spectral diffusion at small times (see Sec. IV) these levels must also satisfy $n_a|2(\Delta^a/E)\gamma_a|[(\Delta_0^a/E)\gamma_a]^2 < \bar{P}|\gamma|\gamma^2$.

As a test of these ideas, consider the case $T = 160$ mK, which we discussed above. At this temperature n_0 is roughly[22] 5.2×10^{32} erg^{-1}cm^{-3}, and Eq. (10b) predicts that n_s is 2.0×10^{32} erg^{-1}cm^{-3}. Thus n_a must account for the difference between n_0 and n_s, which is 3.2×10^{32} erg^{-1}cm^{-3}. In order for these "anomalous" levels to contribute to the specific heat on 1-μsec time scale, we must have $[(\Delta_0^a/E)\gamma_a]^2 \geq 2 \times 10^{-1}\gamma^2$. On the other hand, the condition $n_a[(\Delta_0^a/E)\gamma_a]^2 < \bar{P}\gamma^2$ requires that $[(\Delta_0/E)\gamma_a]^2 < 7 \times 10^{-2}\gamma^2$. The incompatibility of these two conditions indicates that the heat-pulse results are difficult to explain even with anomalous levels present.

Having seen that anomalous levels are only partially successful in explaining specific heat experiments, we will focus throughout this paper on the standard tunneling levels. It is this type of level which determines the interesting ultrasonic properties related to spin-spin interactions.

III. "SPIN-SPIN" COUPLING

As mentioned in Sec. II, the term $D^i\epsilon^i S_z^i$ in Eq. (2) reflects the shift in a "spin's" energy splitting which results from strain fields in the sample. If these strains are due to an ultrasonic pulse, then such a shift leads to relaxational absorption and

dispersion of sound.[4,6] On the other hand, strains may exist in the absence of any external source. Such internal strains lead to interactions among spins as discussed previously by Joffrin and Levelut[12] and Hunklinger and Arnold.[4] These interactions arise because $D^i S^i_z$ is an "elastic-dipole moment" and may be viewed as a source for the strain field just as a magnetic dipole is a source for the magnetic field. By eliminating the strain field, an interaction of the form

$$\mathcal{H}_{\text{spin-spin}} = \sum_{i>j} J_{ij} S^i_z S^j_z \qquad (11)$$

is obtained. The coupling energy is given by

$$J_{ij} = C_{ij}(\Delta^i/E^i)(\Delta^j/E^j)(1/r^3_{ij}) , \qquad (12)$$

where r_{ij} is the distance between spin i and spin j. The quantity C_{ij} depends on the tensor of deformation-potential coupling constants at sites i and j and on the spatial orientation of these tensors (see below).

A comment about this derivation is in order. Interaction terms of the form $S^i_x S^j_x$ could be derived in a similar manner. Such terms have been ignored here because they are unimportant for the applications to be discussed in Secs. V and VI. Their lack of importance is a result of the fact that any two spins can interact through such a term only if they are at resonance with each other. Since the distribution of energy splittings is very large (extreme inhomogenous broadening) the fraction of spins which are at resonance with a given spin is very small compared to the fraction of spins which can interact via Eq. (11). As we shall see in the next section, this latter fraction is determined by the spins which are thermally active ($E^i < 2k_B T$).

In order to estimate the magnitude of J_{ij}, it is necessary to consider the tensor character of the coupling constant γ. For example it can be shown [cf. Eq. (A9)] that J_{ij} vanishes in the case of purely isotropic coupling ($\gamma_{\alpha\beta} = \gamma \delta_{\alpha\beta}$). A general approach is to assume that $\gamma_{\alpha\beta}$ can be decomposed into three eigenvalues with three mutually orthogonal eigenvectors.[17] It is then straightforward to average J_{ij} over (a) the orientation of the three eigenvectors at site j relative to those at site i and (b) the orientation of the unit vector $\hat{r}_{ij}$ relative to the eigenvectors at site i. Such an average is carried out explicitly in the Appendix. There it is shown that the rms average value of J_{ij} is determined by γ^2_l and γ^2_t. By using the value of γ_l obtained from pulse area measurements[11] and the relation $\gamma^2_t \approx \frac{1}{2}\gamma^2_l$ obtained from ultrasonic attenuation experiments,[21] we have derived the estimate [see Eq. (A15)]

$$[\langle C^2_{ij}\rangle]^{1/2} \equiv C_{\text{rms}} = 1.6 \times 10^{-35} \text{ erg cm}^3 . \qquad (13)$$

The quantity $C_{\text{rms}} |\Delta^i \Delta^j| / E^i E^j r^3_{ij}$ is then to be understood [see Eq. (12)] as the average magnitude of the shift in the energy of spin i when spin j flips ($\Delta S^j_z = \pm 1$). The problems of determining r_{ij}, of determining Δ/E, and of estimating errors in our averaging procedure will be discussed in Sec. IV. The smallness of the dimensionless constant $n_s C_{\text{rms}}$, which is less than or equal to 3.2 $\times 10^{-3}$ (using the maximum value of n_s as estimated in Sec. II) guarantees that the energy shift of most spins is only a small fraction of their unperturbed energy splitting E. This enables us to treat the system as a collection of nearly independent spins, ignoring most collective effects.[23]

IV. SPECTRAL DIFFUSION

In this section we begin a discussion of the important dynamical consequences of Eq. (11). The effective Hamiltonian for "spin" i can be written

$$\mathcal{H}^i_{\text{eff}} = E^i_{\text{eff}} S^i_z + B^i \epsilon^i S^i_x , \qquad (14)$$

where

$$E^i_{\text{eff}} = E^i + \sum_{j \neq i} J_{ij} S^j_z . \qquad (15)$$

If the neighboring spins are described by values of S^j_z which are independent of time, their only effect on spin i is a static shift of the energy splitting E^i. Such an effect is, however, quite unobservable because the spectrum of energy splittings in a glass is already much wider (i.e., inhomogeneously broadened) than any static width due to J_{ij} (cf. comment at the end of Sec. III). Thus any static shifts can be assumed to have been incorporated into the definition of E^i.

On the other hand, if S^j_z is a time-dependent quantity, no simple redefinition of E^i will suffice. Interesting effects then arise wherein E^i_{eff} changes during the course of an experiment. The possibility of such fluctuations in resonant frequency was first mentioned by Hunklinger and Arnold in connection with ultrasonic saturation experiments.[4] In order to treat this time-dependent effect, we introduce the concept of spectral diffusion[13] in glasses.

We focus our attention on a test spin at site i, which has an energy splitting $E^i_{\text{eff}} = \hbar\omega_0$ at time $t = 0$. In the standard terminology for spectral diffusion,[13,24] this test spin is known as an "A spin." In general the A spins are distinguished from all the other spins ("B spins") by having values of ω_0 roughly equal to the frequency of the ultrasonic pulse in a spin-echo or saturation experiment. In an inhomogeneously broadened spectrum, B spins will generally outnumber A spins. As time pro-

gresses and B spins flip, the A-spin energy split-
ting E^i_{eff} will wander away from $\hbar\omega_0$. To describe
this process, we define the spectral diffusion ker-
nal[13,24] $D(\omega - \omega_0, t)$. This function is defined so
that $D(\omega - \omega_0, t)d\omega$ is the probability that spin i has
acquired an energy splitting $E^i_{eff} = \hbar\omega$ at time t.
For dipolar interactions it is an established re-
sult that the spectral diffusion kernel has the ap-
proximate form[13,24]

$$D(\omega - \omega_0, t) = \frac{1}{\pi} \frac{\Delta\omega(t)}{(\omega - \omega_0)^2 + [\Delta\omega(t)]^2} . \qquad (16)$$

The diffusion width $\Delta\omega(t)$ is proportional to $\langle|J_{ij}|\rangle$
with r_{ij}^{-3} replaced by $n_f(t)$, the density of B spins
which have flipped during the interval t. The ef-
fects of all neighboring spins (not just nearest
neighbors) are included, assuming that they are
distributed at random in the sample. The result
of the standard calculation for the width is[13,24]

$$\Delta\omega(t) = \frac{2\pi^2}{3} \frac{C_{rms}}{\hbar} \left\langle\left|\frac{\Delta}{E}\right|\right\rangle_A \left\langle\left|\frac{\Delta}{E}\right| n_f(t)\right\rangle_{E,\lambda} . \qquad (17)$$

The average[25] $\langle|\Delta/E|\rangle_A$ refers to the A spins,
whose time-dependent energy splittings have the
experimental consequences discussed in Secs. V
and VI. As mentioned above, these spins are in
resonance with an ultrasonic pulse and thus have
energy splittings E which are constrained to lie
near the pulse frequency. The average
$\langle|\Delta/E| n_f(t)\rangle_{\lambda,E}$ refers to the numerically superior
B spins whose flipping leads to spectral diffusion.
Since these spins are not in resonance with an
ultrasonic pulse, we must include contributions
from B spins with all energy splittings E.

We should note that expression (17) for $\Delta\omega(t)$
represents an upper bound to the actual value of
$\Delta\omega(t)$. This is the case because in deriving Eq.
(17) from Eq. (12), we have replaced the exact
quantity $\langle|C_{ij}|\rangle$ by the tractable quantity $[\langle C_{ij}^2\rangle]^{1/2}$,
which we call C_{rms} [see Eq. (A11)]. Estimates
based upon the simpler case of a true electric di-
pole suggest that the actual width is roughly 85%
of the rms upper bound value [cf. Eq. (A12)].

The next step is to calculate $n_f(t)$, the spatial
density of flipped B spins. To be more precise,
$n_f(t)$ is the density of B spins which have flipped
an odd number of times. In this discussion we
make the plausible assumption that all flipping re-
sults from contact with a bath of thermal phonons.
Recall that direct phonon absorption and emission
processes lead to spin-phonon relaxation at the
rate given by Eq. (9). The same processes con-
trol the rate at which S_z^j fluctuates (flips) in ther-
mal equilibrium. Simple rate equations predict
that for B spins with a fixed value of E and λ, the
contribution to $n_f(t)$ is

$$dn_f(E, \lambda, t) = \tfrac{1}{2} n(E, \lambda) \operatorname{sech}^2(E/2k_B T)$$
$$\times (1 - e^{-t/T_1(E,\lambda)}) \, dE \, d\lambda , \qquad (18)$$

where $n(E, \lambda)$ is the spatial density of such spins.
The factor $\operatorname{sech}^2(E/2k_B T)$ restricts consideration
to those B spins with small enough energy split-
tings so as not to be frozen into their ground
states.

The final result is now obtained by integrating
Eq. (18) over E and λ, using $\bar{P}$ and the "standard"
tunneling level assumptions of Sec. II to deter-
mine $n(E, \lambda)$. The result of such a calculation
when substituted into Eq. (17) is

$$\Delta\omega(t, T) = \Delta\omega(t = \infty, T) \frac{1}{2(\eta - \ln 2)}$$
$$\times \int_0^\infty dx \operatorname{sech}^2 x \int_{4e^{-2\eta}}^1 \frac{dr}{r} (1 - e^{-rT_1^{-1}(x)t}) , \qquad (19)$$

where $x \equiv E/2k_B T$ and $r \equiv \exp[-2(\lambda - \lambda_{min})]$. The
quantity $T_1^{-1}(x)$ is the maximum B-spin flipping
rate for a particular value of $E(= 2xk_B T)$. Using
the coupling constant estimates discussed prior to
Eq. (13) and in Sec. II B, we derive $T_1^{-1}(x)$
$= 960 T^3 x^3 \coth x \ \mu\text{sec}^{-1}$ from Eq. (9). The integral
over r takes into account the dependence of
$n(E, \lambda), T_1$, and $|\Delta/E|$ upon λ when E is fixed.
Equation (19) has been written in such a way as
to explicitly indicate that $\Delta\omega$ approaches a limit
as $t \to \infty$ whenever $\eta < \infty$. This limit can be under-
stood by noting that for long times half of the ther-
mally active $(E \lesssim 2k_B T)$ B spins have flipped an odd
number of times. This fact leads to a final width
proportional to T given by

$$\Delta\omega(t = \infty, T) = \frac{2\pi^2}{3} \frac{1}{\hbar} C_{rms} \left\langle\left|\frac{\Delta}{E}\right|\right\rangle_A (\eta - \ln 2) \bar{P} k_B T . \qquad (20)$$

Using the value of C_{rms} from Eq. (13), the value[25]
$\langle|\Delta/E|\rangle_A = \tfrac{1}{2}$, and the value of $\bar{P}$ derived in Sec.
II, we estimate that $(2\pi)^{-1}\Delta\omega(t = \infty, T)$
$= 23(\eta - \ln 2)T$ MHz with T measured in degrees.
A spectral width of this magnitude with $\eta \approx 10$ is
in reasonable agreement with experiment as will
be seen in Secs. V and VI.

The important new feature of this calculation is
that $\Delta\omega$ increases monotonically with time. For
short times $(t \ll T_1)$ the probability that a neigh-
boring B spin has flipped once is proportional to t,
which allows us to evaluate Eq. (19) explicitly as

$$\Delta\omega(t, T) = \Delta\omega(t = \infty, T) \frac{1}{2(\eta - \ln 2)}$$
$$\times \int_0^\infty t T_1^{-1}(x) \operatorname{sech}^2 x \, dx$$
$$= \Delta\omega(t = \infty, T) \frac{1}{2(\eta - \ln 2)} \frac{\pi^4}{64} 960 T^3 t . \qquad (21a)$$
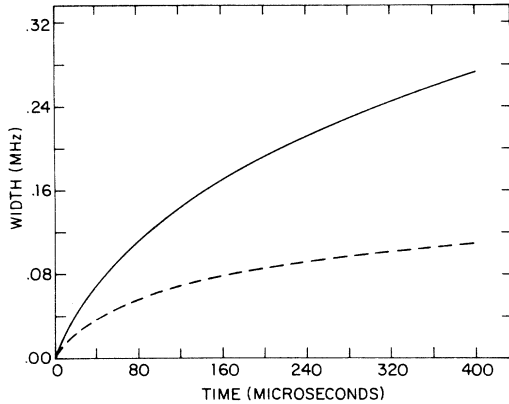
FIG. 3. Spectral diffusion width $(2\pi)^{-1}\Delta\omega(t,T)$ from Eq. (19) at a temperature of 20 mK. Solid curve corresponds to $\eta > 5$; dashed curve is for $\eta = 1$.

When t is measured in microseconds and T is measured in degrees, we obtain

$$(2\pi)^{-1}\Delta\omega(t, T) = 1.7 \times 10^4 T^4 t \text{ MHz} \tag{21b}$$

in this short-time limit. For longer times $\Delta\omega(t, T)$ rises more slowly than linearly in t as B spins undergo multiple flips.

The behavior of $\Delta\omega(t, T)$ in the regime intermediate to Eqs. (20) and (21) is shown in Figs. 3–5 for various values of T and η. In these curves it is evident that the time scale varies as T^{-3} and the $\Delta\omega$ scale varies as T. The dependence upon η is more complicated. At small times there is virtually no η dependence because $\Delta\omega$ is determined by the B spins which flip fastest $(\lambda \approx \lambda_{min})$, whose density is given by $\bar{P}$. For longer times the slower spins begin to have an effect. These B spins with $\lambda_{min} < \lambda < \lambda_{max}$ lead to a long-time tail, causing $\Delta\omega$ to rise very slowly as $\ln t$. This slow rise has the same origin as the $\ln t$ behavior predicted for the "standard" level specific heat.[14] This rising stops when B spins with $\lambda = \lambda_{max}$ have begun to flip. The observation that larger values

FIG. 5. Spectral diffusion width $(2\pi)^{-1}\Delta\omega(t,T)$ at 500 mK. Solid curve is for $\eta = 10$; dotted curve is for $\eta = 5$; dashed curve is for $\eta = 1$.

of η imply longer periods of slow rise explains why curves with different values of η are more easily distinguished at long times.

V. PHONON ECHO DECAY

The recent observation of phonon echoes in fused silica[11] constitutes a powerful tool for studying the dynamics of the two-level systems ("spins"). Echoes occur when a series of phonon pulses in resonance with a small fraction of the spins (i.e., the A spins) leads to coherent emission of ultrasonic radiation by these spins. The mechanism is the same as in NMR echoes,[26] ESR echoes,[24] and photon echoes.[27] In a two-pulse echo sequence (see Fig. 6), the first pulse puts the A spin labeled by i into a nonstationary state, causing it to precess at its resonant frequency $\omega^i = \hbar^{-1}E^i$. As this free precession occurs, the spin emits ultrasonic radiation. This signal soon dies, however, because the large spread in precessional frequencies leads to a rapid loss of phase coherence among the A spins. If a second pulse which reverses the direction of precession is applied at time τ after the first pulse, the spins will retrace their various accumulations of phase. At a time 2τ after the first pulse, the A spins will all have the same phase, and the resulting ultrasonic radiation can be detected. Three-pulse
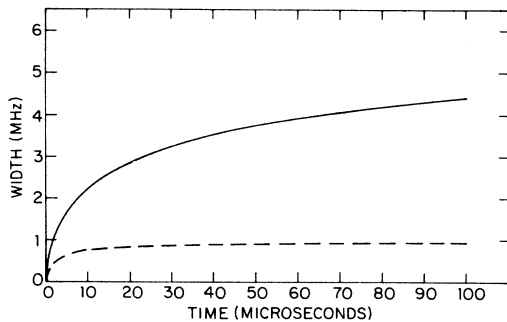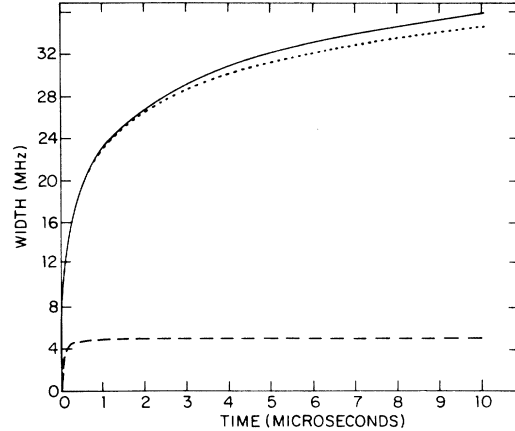
FIG. 4. Spectral diffusion width $(2\pi)^{-1}\Delta\omega(t,T)$ at 100 mK. Solid curve is for $\eta > 5$; dashed curve is for $\eta = 1$.
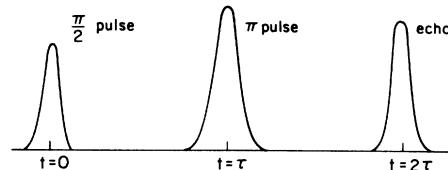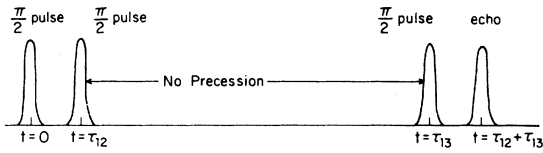
FIG. 6. Two-pulse (spontaneous) echo sequence.

FIG. 7. Three-pulse (stimulated) echo sequence, showing the long interval during which no precession of the A spins occurs.

echoes[24] result from a modified two-pulse sequence in which the second pulse is split into two parts separated by a time interval during which no precession occurs (see Fig. 7).

A. Two-pulse echoes

Much information can be gained by observing the amplitude of an echo signal as a function of the time intervals between the pulses. Such dependence occurs only when some mechanism interferes with the phase cancellation discussed above. A static line broadening, of course, is not capable of causing such interference. On the other hand, a dynamic effect such as spectral diffusion can have dramatic consequences. The key concept connecting phonon echoes and spectral diffusion is the loss of phase coherence which occurs when the precessional frequency of an A spin changes during the course of an echo experiment. For a two-pulse sequence the resulting echo amplitude is given by[13,24,28,29]

$$E(2\tau) = \left\langle \exp\left(i \int_0^\tau dt\,\omega(t) - i \int_\tau^{2\tau} dt\,\omega(t)\right)\right\rangle, \quad (22)$$

where $\langle \cdots \rangle$ devotes an average over all A spins and over all flip histories of their B-spin neighbors. In the limit that τ is much less than the shortest thermal $(E \lesssim 2k_BT)$ B-spin T_1 [cf. Eq. (21a)], the small-time limit of the spectral diffusion kernel yields the result first derived by Klauder and Anderson[13]

$$E(2\tau) = e^{-m\tau^2}, \quad (23a)$$

where

$$m \equiv \lim_{t \to 0} t^{-1}\Delta\omega(t, T). \quad (23b)$$

As we shall see below, there is good reason to believe that this small-time limit applies to the actual experiments on glasses. Nevertheless it is useful to understand the qualitative features of $E(2\tau)$ for longer times. Hu and Hartmann[28] have derived $E(2\tau)$ with no restrictions on τ for the case of B spins with a single flipping rate and an equal probability of being "up" or "down." Since the glass problem allows a wide distribution of rates [cf. Eqs. (9) and (19)] and also has B spins

which are more likely to be down than up, a similar derivation of a general $E(2\tau)$ for glasses is nontrivial. The general features of Hu and Hartmann's solution will, however, apply to glasses. These features are (a) a regime of short times where (23) applies, (b) a crossover region in which $E(2\tau)$ falls off more slowly than $\exp(-m\tau^2)$ and has a roughly exponential decay bounded from below by $\exp(-\pi^{-1/3}mT_1\tau)$, and (c) a long-time limit in which $E(2\tau)$ falls off slowly as $\exp(-8^{1/2}\pi^{-1/2}T_1^{3/2}m\tau^{1/2})$.

In making estimates of the echo envelope function $E(2\tau)$, we have used the coupling constants values which led to Eq. (21b). These same coupling constants permit the evaluation of B-spin flipping times as was discussed following Eq. (19). For example at $T = 20$ mK the minimum flipping time for B spins with $E = 2k_BT$ is found to be 99 μsec. This time decreases at T^{-3}, becoming roughly 1.6 μsec at 80 mK. Another important time, which is distinct from a B-spin flipping time, is the time required for an A spin (i.e., a direct contributor to the echo) to relax to thermal equilibrium. This particular time is given by Eq. (9) with E determined by the ultrasonic frequency $(E = \hbar\omega)$. For A spins resonant with a 0.68-GHz pulse, the minimum relaxation time $(\lambda = \lambda_{\min})$ at 20 mK (80 mK) is 160 μsec (49 μsec). In view of the fact that the two-pulse experiments in Ref. 11 have a maximum duration of roughly 15 μsec at 20 mK, it appears unlikely that this direct relaxation of the A spins contributes to the observed echo decay. Furthermore the magnitude of the B-spin flipping time suggests that the small-time approximation for the spectral diffusion mechanism [cf. Eq. (23a)] should be reasonable. Using Eq. (21b) this theory predicts that

$$m = 1.1 \times 10^5 T^4 \,\mu\text{sec}^{-2}. \quad (24)$$

If we define the phase-memory time T_2' as the time 2τ in which the echo envelope falls to $1/e$, we find, using the estimate (24),

$$T_2' = 6.0 \times 10^{-3}T^{-2} \,\mu\text{sec}. \quad (25)$$

Experimental results for two-pulse echoes at 0.68 GHz in Suprasil W yield values of T_2' equal to 14 and 3 μsec at $T = 20$ mK and $T = 45$ mK, respectively.[11] The corresponding theoretical predictions from Eq. (25) are 15 and 3.0 μsec. The agreement between theory and experiment in both the magnitude and the temperature dependence of T_2' is remarkably good. We should mention, however, that the experiments show a more nearly exponential decay in $E(2\tau)$ as opposed to the Gaussian shape predicted by Eq. (23a). Furthermore some frequency dependence of T_2' is observed above 0.68 GHz, and this is difficult to understand in terms of

spectral diffusion.[30] At first glance such fre-
quency dependence suggests that direct relaxation
of the A spins is occurring, but an A-spin T_1 on
the order of 15 μsec is extremely difficult to rec-
oncile with the observation of three-pulse echoes
at times exceeding 100 μsec (Ref. 30) (see below).
It is more likely that these difficulties are related
to the presence of pulse attenuation during the
echo sequence. Such attenuation is known to oc-
cur[11] and to be frequency dependent.[21] The agree-
ment we have found with experimental measure-
ments of T_2' can be interpreted as an independent
check on Golding and Graebner's determination of
the coupling tensor γ, from their pulse area mea-
surements.[11] Note that our rms averaging pro-
cedure tends to overestimate m [see the discus-
sion following Eq. (17)] and thus to underestimate
T_2'. Lowering m by 15% increases T_2' by 10% and
slightly diminishes the agreement between theory
and experiment.

B. Three-pulse echoes

We turn now to the three-pulse echoes, a good
discussion of which has been given by Mims.[24,31]
For this sequence the echo envelope is given
by[13,24,28,29] (see Fig. 7)

$$F(\tau_{13}, \tau_{12}) = \exp[-(\tau_{13} + \tau_{12})/T_1] E_s(\tau_{13}, \tau_{12}) , \quad (26a)$$

where

$$E_s(\tau_{13}, \tau_{12}) = \left\langle \exp\left(i \int_0^{\tau_{12}} dt \, \omega(t) - i \int_{\tau_{13}}^{\tau_{13}+\tau_{12}} dt \, \omega(t) \right) \right\rangle .$$

$$(26b)$$

In Eq. (26a), the first factor results from direct
A-spin relaxation, a process which we neglected
for two-pulse echoes but which may be important
for three-pulse echoes (see below). The second
factor in (26a), $E_s(\tau_{13}, \tau_{12})$, is the spectral diffu-
sion contribution to three-pulse decay and is the
analog of $E(2\tau)$ in Eq. (22). It is apparent that
during the intervals $0 < t < \tau_{12}$ and $\tau_{13} < t < \tau_{13} + \tau_{12}$
the echo amplitude $E_s(\tau_{13}, \tau_{12})$ decays as a result
of simultaneous precession and spectral diffusion
just as in the two-pulse sequence. The interval
$\tau_{12} < t < \tau_{13}$, however, introduces a new feature:
spectral diffusion in the absence of spin preces-
sion. Since no phase is accumulated, the effect of
spectral diffusion in this interval is to contribute
an effectively static line broadening $\Delta\omega(T, \tau_{13}$
$- \tau_{12})$. This broadening leads to additional decay
as the spins precess in the interval $\tau_{13} < t < \tau_{13} + \tau_{12}$
just as static line broadening causes decay of a
free precession signal.[26] When $\tau_{12} \ll T_1$, this de-
cay mechanism leads to a factor in the expression
for $E_s(\tau_{13}, \tau_{12})$ which is the result of the Fourier
transform of the diffusion kernel[31] [cf. Eq. (16)]

$$E_s(\tau_{13}, \tau_{12})/E(2\tau_{12}) = \exp[-\tau_{12}\Delta\omega(\tau_{13} - \tau_{12}, T)] . \quad (27)$$

This factor can be seen explicitly in the standard
expression for the short-time limit[13,28] (τ_{12}, τ_{13}
$\ll T_1$):

$$E_s(\tau_{13}, \tau_{12}) = \exp(-m\tau_{12}\tau_{13})$$
$$= \exp(-m\tau_{12}^2)\exp[-\tau_{12}m(\tau_{13} - \tau_{12})] , \quad (28)$$

where $\Delta\omega(\tau_{13} - \tau_{12}, T) = m(\tau_{13} - \tau_{12})$ and $\exp(-m\tau_{12}^2)$
is recognized as the two-pulse envelope $E(2\tau_{12})$
in Eq. (27). Furthermore for arbitrary values of
$\tau_{13} - \tau_{12}$ with $\tau_{12} \ll T_1$ the validity of Eq. (27) has
been established by Hu and Hartmann for the case
of a single B-spin flipping rate.[28] Extension to
the glass problem follows the arguments preceding
Eq. (27) and the discussion of spectral diffusion
by Mims.[31]

In the three-pulse experiments we are typically
in the regime where τ_{12} is sufficiently small so
that Eq. (27) applies with the added simplification
$E(2\tau_{12}) \approx 1$. For example Golding and Graebner
report preliminary results at 20 mK in which
$\tau_{12} \approx 1$ μsec and $\tau_{13} \approx 100$ μsec.[30] The curves for
$\Delta\omega(t, T)$ discussed in Sec. IV show that $E_s(\tau_{13}, \tau_{12})$
should fall exponentially only for small values of
τ_{13}. For longer times the envelope factor
$E_s(\tau_{13}, \tau_{12})$ should fall more slowly, eventually
ceasing to decline. [Note, however, that
$F(\tau_{13}, \tau_{12})$ in Eq. (26a) will continue to decline as
a result of A-spin T_1 processes.] These qualita-
tive features of $E_s(\tau_{13}, \tau_{12})$ are exhibited by the
theoretical curves in Figs. 8 and 9 for various
values of T, η, and τ_{12}. Such nonexponential τ_{12}-
dependent decay has been observed recently in
three-pulse experiments.[30] To facilitate com-
parison with experiment, we show in Fig. 10 a
decay time $(T_1')_{sd}$ defined as that value of $\tau_{13} - \tau_{12}$
at which $E_s(\tau_{13}, \tau_{12})$ falls to e^{-1} if we set $E(2\tau_{12}) = 1$.
For T below about 20 mK and $\eta \leq 10$, $(T_1')_{sd}$ be-
comes very long as the $\Delta\omega(t, T)$ curves level off
for large times. The computed values of $(T_1')_{sd}$
all occur in the nonexponential region, where the
flatness of the echo envelope will make an experi-
mental determination of $(T_1')_{sd}$ uncertain.

Values of T_1 for A spins resonant at a frequency
of 0.68 GHz are also shown in Fig. 10. These val-
ues are derived from Eq. (9) with $\lambda = \lambda_{min}$, using
the coupling constant values ($\gamma_l = 1.6$ eV, $\gamma_t^2 \approx \frac{1}{2}\gamma_l^2$)
discussed in Sec. II B. It is important to note that
the condition $\tau_{13} < T_1$ may not hold for the values
of τ_{13} shown in Figs. 8–10. When $\tau_{13} \gtrsim T_1$, direct
relaxation of the A spins will make a τ_{12}-indepen-
dent contribution to the three-pulse echo decay
when $\tau_{12} \ll \tau_{13}$ [cf. Eq. (26a)]. As is evident in
Fig. 10, this process eventually causes a decay
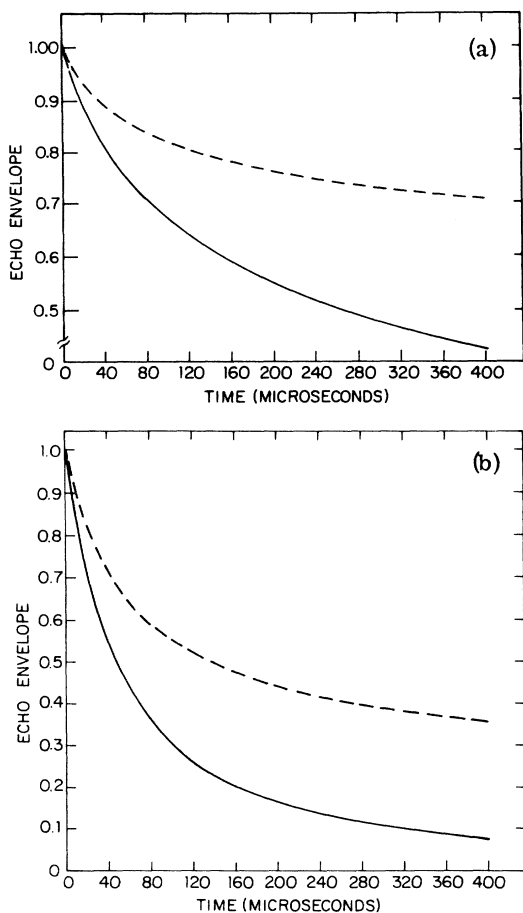which is faster than spectral diffusion as T de-

FIG. 8. Theoretical three-pulse spectral diffusion decay envelopes $E_s(\tau_{13}, \tau_{12})$ given by Eq. (27) when $\tau_{12} \ll T_1$. The temperature is 20 mK. Solid curves are for $\eta = 10$; dashed curves are for $\eta = 1$. (a) $\tau_{12} = 0.5\,\mu$ sec; (b) $\tau_{12} = 1.5\,\mu$ sec.

creases. Thus the observed decay time $(T_1')_{\mathrm{obs}}$ should be roughly equal to the lower of the two curves in Fig. 10 [i.e., $(T_1')_{\mathrm{obs}}^{-1} \approx (T_1)_A^{-1} + (T_1')_{sd}^{-1}]$. It should be emphasized again that the experimentally observed inequality $T_2' \ll (T_1')_{\mathrm{obs}}$ cannot be understood in terms of A-spin T_1 processes alone. A strong argument in favor of spectral diffusion decay is that it allows the two-pulse decay time T_2' to be much shorter than both the A-spin T_1 and the three-pulse decay time $(T_1')_{\mathrm{obs}}$. Furthermore spectral diffusion decay yields echo envelopes which depend parametrically on τ_{12} in agreement with preliminary experimental results.[30]

VI. SATURATION AND RECOVERY

A. Saturation

Another type of experiment to which spectral diffusion applies is saturation of the "spins" by
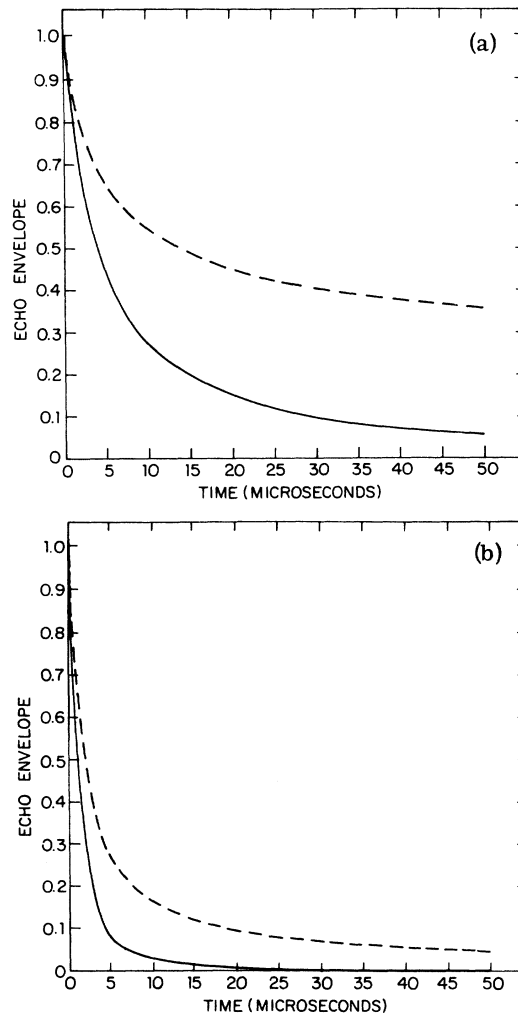

FIG. 9. Theoretical three-pulse spectral diffusion decay envelopes $E_s(\tau_{13}, \tau_{12})$ given by Eq. (27) when $\tau_{12} \ll T_1$. The temperature is 50 mK. Solid curves are for $\eta = 10$; dashed curves are for $\eta = 1$. (a) $\tau_{12} = 0.5\,\mu$sec; (b) $\tau_{12} = 1.5\,\mu$sec.

an ultrasonic pulse. In Eq. (8) the factor $\tanh(\hbar\omega / 2k_B T)$ represents the difference (in thermal equilibrium) between the number of "up" spins and the number of "down" spins with energy splitting $E = \hbar\omega$. Any reduction in this population difference resulting from a strong ultrasonic pulse leads to a decrease in the attenuation of that pulse and of subsequent pulses.[4-6] This phenomenon is closely related to self-induced transparency,[32] in which a coherent time-dependent variation of the population difference leads to pulse shaping, pulse delay, and anomalously low attenuation.

In order to treat saturation effects, we introduce phenomenological Bloch equations[4,5,12]

$$\frac{dM_x(\omega')}{dt} = -\omega' M_y(\omega') - T_2^{-1} M_x(\omega') , \qquad (29a)$$
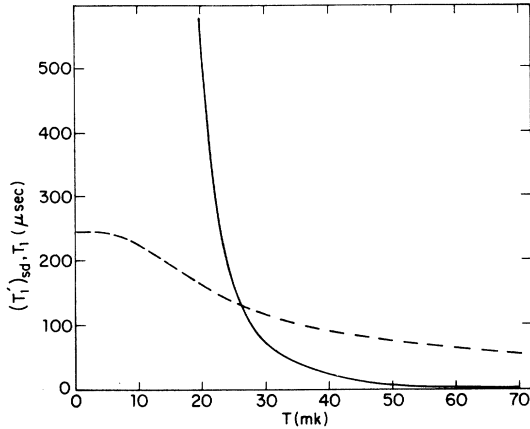
FIG. 10. Theoretical temperature dependence of three-pulse echo decay time. Solid curve is the value of $(T'_1)_{sd}$ calculated from Eq. (27) with $\tau_{12} \ll T_1$. This curve was calculated with $\eta = 10$ and $\tau_{12} = 0.5$ μsec. The dashed curve is T_1 with $\lambda = \lambda_{min}$ for A spins at resonance with a 0.68-GHz ultrasonic pulse.

$$\frac{dM_y(\omega')}{dt} = \omega' M_x(\omega') + \frac{B\epsilon}{\hbar} M_z(\omega') - T_2^{-1} M_y(\omega') \, ,$$

(29b)

$$\frac{dM_z(\omega')}{dt} = -\frac{B\epsilon}{\hbar} M_y(\omega') - T_1^{-1}(\omega')$$

$$\times [M_z(\omega') - M_z^0(\omega')] \, ,$$ (29c)

where[25] $\vec{M}(\omega') \equiv \langle \vec{S}^i \rangle_A$ with the constraint $E^i = \hbar\omega'$. In this definition we have explicitly displayed the resonant frequency ω' as a reminder that we are dealing with an inhomogeneously broadened spectrum. Thus $\vec{M}(\omega')$ corresponds to those A spins in a "spin packet" centered at ω' with a homogeneous width T_2^{-1}. Furthermore, $\vec{M}(\omega')$ is obtained from $\vec{S}^i$ by an average which is weighted in favor of those A spins which are strongly coupled to ultrasonic pulses.[25] The "spin-lattice" relaxation time $T_1^{-1}(\omega')$ for such spins is given by Eq. (9) with $\lambda \approx \lambda_{min}$ and $E = \hbar\omega'$. The quantity $-2M_z^0(\omega') = \tanh(\frac{1}{2}\beta\hbar\omega')$ is the population difference for spins in thermal equilibrium with the "lattice." The free precession terms proportional to $\pm\omega'$ and $B\epsilon/\hbar$ in Eqs. (29) follow from Eqs. (1) and (2). The strain field ϵ is a time-dependent quantity which oscillates at the ultrasonic pulse frequency, ω. That is,

$$\epsilon = \epsilon(t) = \mathrm{Re}(\epsilon_0 e^{-i\omega t}) \, ,$$

where ϵ_0 is related to the energy density $\mathcal{E}$ (per unit volume) in the ultrasonic pulse, by

$$\mathcal{E} = \frac{1}{2}\rho c_\alpha^2 \epsilon_0^2 \quad (\alpha = l, t) \, .$$ (30)

The energy density is related in turn to the average

pulse energy flux $(\phi = \mathcal{E}c_\alpha)$ and to the areal energy density $(E_0 = \mathcal{E}c_\alpha\tau_p)$, where τ_p is the pulse duration.

To date, most theoretical treatments of saturation in glasses have employed the steady-state solutions of Eqs. (29) in the reference frame rotating about the z axis at frequency ω.[4,5,12] The steady-state energy absorption from each "spin packet" is then summed over the inhomogeneous distribution of ω', just as in the saturation theory of Portis.[33] This theory leads to saturation when the factor $(B\epsilon_0/2\hbar)^2 T_1 T_2$ exceeds unity. The phonon mean free path falls off as $[1 + (B\epsilon_0/2\hbar)^2 T_1 T_2]^{-1/2}$ and the absorption line is power broadened to a width given by $T_2^{-1}[1 + (B\epsilon_0/2\hbar)^2 T_1 T_2]^{1/2}$.

There are several difficulties with using steady-state solutions of Eqs. (29) to describe the saturation process in glasses. One such difficulty is that the pulse length τ_p is generally much shorter than the estimated value of T_1 for the A spins (spins resonant with pulses). For example, based on our coupling constant estimates (cf. Sec. II B), T_1 for $\omega'/2\pi = 0.68$ GHz and $\lambda = \lambda_{min}$ ranges from 7.8 μsec at $T = 500$ mK to 160 μsec at $T = 20$ mK (cf. Fig. 10). On the other hand, experimental values of τ_p rarely exceed 1 μsec.[4,5] Thus it appears unlikely that the vector $\vec{M}(\omega')$ in Eqs. (29) has sufficient time during an ultrasonic pulse to reach a steady-state value. The inequality $\tau_p \ll T_1$ suggests that a time-dependent approach similar to that employed in the theory of self-induced transparency[32] is more appropriate than steady-state saturation theory.

A second difficulty related to Eqs. (29) is the question of what to use for T_2^{-1}. For a simple homogeneously broadened line, T_2 is the "dephasing time" and yields the linewidth, the free precession decay time, and the spin-echo decay time.[26] For an inhomogeneously broadened line, as we have in glasses, T_2^{-1} no longer represents the total linewidth. Instead T_2^{-1} is the width of a "spin-packet,"[13,33] which is a subset of the spins characterized by a common resonant frequency (i.e., the A spins are a spin packet). A weak ultrasonic pulse with a well-defined frequency ω will affect $\vec{M}(\omega')$ only for those values of ω' lying roughly between $\omega - T_2^{-1}$ and $\omega + T_2^{-1}$. In this context T_2 remains a "dephasing time" and yields an estimate of the spin-echo decay time.

It should now be clear that spectral diffusion is potentially a major contributor to the phenomenological parameter T_2^{-1}, viewed as a dephasing time and as a spin-packet width. Certainly the dephasing due to spectral diffusion leads to spin-echo decay (cf. Sec. V). Furthermore the width of a spin packet obviously depends on the diffusion

of spins in frequency space. The difficulty associated with T_2^{-1} stems from the fact that spin-echo decay is not a simple exponential process and that the spectral diffusion spin-packet width $\Delta\omega(t)$ (cf. Sec. IV) is a function of time. Thus no single time-independent parameter, such as T_2^{-1}, can possibly describe the dephasing and spin-packet width resulting from spectral diffusion. Consequently the suggestion[12] that spin-spin interactions can be incorporated into a time-independent T_2^{-1} must be viewed with some caution.

Unfortunately there exists no complete theory to describe the dynamics of saturation in the presence of the type of spectral diffusion we have been discussing. Some progress has been made in describing steady-state saturation in the presence of cross-relaxation (another type of "spectral diffusion" associated with energy transfer rather than resonant frequency shifts).[34,35] In more closely related work, Wolf[36] has developed a theory for steady-state saturation in the presence of *large* resonant frequency shifts due to spatial diffusion of spins. In his theory the spin-packet width eventually equals the full inhomogeneous linewidth as the rate of diffusion increases.

In the absence of a complete theory, we wish to retain the essential features of Eqs. (29) by defining an effective spin-packet width T_2^{-1}. Of course one contribution to T_2^{-1} is T_1^{-1}, which represents a lifetime broadening due to the uncertainty principle. In order to estimate the spectral diffusion contribution to T_2^{-1}, we make the plausible assumption that spectral diffusion occurs for a time interval equal to the ultrasonic pulse duration τ_p. Thus

$$T_2^{-1} \approx T_1^{-1} + \Delta\omega(\tau_p, T). \tag{31}$$

We are now in a position to make an estimate of T_2^{-1} with $\eta = 10$ for a spin packet (i.e., A spins) at resonance with an ultrasonic pulse of frequency $\omega/2\pi = 0.68$ GHz and duration $\tau_p = 1$ μsec. The two terms contributing to T_2^{-1} are shown in Table I for various values of the temperature. It is apparent that spectral diffusion is the dominant broadening mechanism in Eq. (31), becoming more dominant at higher temperatures.

We now wish to apply the phenomenological theory of Eqs. (29) to actual ultrasonic experiments, using estimates of T_1 and T_2 such as are shown in Table I. One interesting issue, to which we have already alluded, is the question of the relative magnitudes of T_1, T_2, and τ_p. We have already seen that $\tau_p \ll T_1$ and that $T_2 \ll T_1$. From Table I it is apparent that $T_2 < \tau_p$ for temperatures above roughly 50 mK and that $T_2 > \tau_p$ for temperatures below roughly 50 mK. Thus below 50 mK, τ_p is shorter than both T_1 and T_2, a situation which is

TABLE I. Two contributions to the spin packet width in Eq. (31). T_1^{-1} is calculated for $\omega'/2\pi = 0.68$ GHz. The values of $\Delta\omega(\tau_p, T)$ come from Figs. 3–5 with $\tau_p = 1$ μsec and $\eta = 10$.

T (mK)	T_1^{-1} (μsec^{-1})	$\Delta\omega(\tau_p, T)\left(\dfrac{\Delta\omega(\tau_p, T)}{2\pi}\right)$
500	0.13	150 μsec^{-1} (24 MHz)
100	2.6×10^{-2}	4.7 μsec^{-1} (0.75 MHz)
20	6.2×10^{-3}	1.5×10^{-2} μsec^{-1} (2.4 KHz)

favorable to self-induced transparency.[32] Above 50 mK we have $T_2 < \tau_p < T_1$, a situation in which neither self-induced transparency nor steady-state saturation is likely to occur. This is a regime of noncoherent transient saturation.

A second experimental issue is the width of the "burned hole" created by a strong saturating pulse.[4,37] For the moment we will be concerned only with the initial width of the hole, a quantity which we will call δ. We defer any consideration of what happens to the hole width at later times (after the pulse is turned off) to the discussion of saturation recovery (see below). We have already discussed some of the contributions to the initial hole width δ. The spin-packet width $T_2^{-1} \approx \Delta\omega(\tau_p, T)$ is one such contribution. The frequency uncertainty in the ultrasonic pulse, given by τ_p^{-1}, also contributes to δ. Finally, the magnitude ϵ_0 of the saturating field $\epsilon(t)$ [cf. Eqs. (29) and (30)] can influence the frequency range over which the burned hole extends.[38] For example at a "typical"[4,21] saturating ultrasonic energy per area, $E_0 = 5 \times 10^{-5}$ erg/cm^2, we find that $\epsilon_0 = 1.5 \times 10^{-8}$ using $c_l = 5.8 \times 10^5$ cm/sec and $\rho = 2.2$ g/cm^3 in Eq. (30). This strain corresponds to a frequency $\omega_1 \equiv \epsilon_0 B/2\hbar = \epsilon_0 \gamma_l/\hbar$, using Eq. (5). For $\gamma_l = 1.6$ eV, we obtain $\omega_1 = 38$ μsec^{-1} ($\omega_1/2\pi = 6$ MHz). Likewise for $c_t = 3.8 \times 10^5$ cm/sec and $\gamma_t = 1.1$ eV, we obtain $\omega_1 = 50$ μsec^{-1} ($\omega_1/2\pi = 8$ MHz).

Comparison with values of T_2^{-1} from Table I and with $\tau_p^{-1} = 1$ μsec^{-1} leads us to believe that δ is most strongly influenced by T_2^{-1} at higher temperatures ($T \gtrsim 200$ mK) and by "power broadening" (ω_1) at lower temperatures ($T \lesssim 200$ mK). Hunklinger and Arnold have reported a power-independent width $\delta/2\pi \approx 50$ MHz at $T = 550$ mK in borosilicate glass.[4] These results are in rough accord with the value $(2\pi T_2)^{-1} \approx 24$ MHz obtained from Table I. Nevertheless it must be kept in mind that the theoretical hole width will exceed 24 MHz if we allow spectral diffusion to take place for a time longer than the pulse width, $\tau_p = 1$ μsec. Consideration of spectral diffusion after the pulse has been turned off brings us naturally to the subject of saturation recovery.

B. Saturation recovery

Let us consider the recovery of $M_z(\omega')$ toward $M_z^0(\omega')$ following a saturating pulse at frequency ω. Here we ignore the details of the saturation process itself and simply assume that the pulse "burns a hole" in $M_z(\omega')$ at $t = 0$ as shown by the solid curve in Fig. 11. The subsequent change as $M_z(\omega')$ recovers can be measured by observing the changes in the ultrasonic attenuation of a nonsaturating pulse with frequency ω' at a later time t. The width of a hole in $M_z(\omega')$ can be determined by varying the probe frequency ω'.

As an illustrative example we assume that the saturating pulse at frequency ω depresses $M_z(\omega')$ according to the idealized expression[38]

$$M_z(\omega', t = 0) = M_z^0(\omega) \frac{(\omega' - \omega)^2}{(\omega' - \omega)^2 + \delta^2} , \qquad (32)$$

where δ is the initial hole width, which depends on the details of the saturation process discussed above. Equation (29c) with $\epsilon = 0$ describes the thermal relaxation (A-spin T_1) contribution to the recovery of $M_z(\omega')$, a process in which the pattern expressed by Eq. (32) simply disappears in time T_1 without further broadening. If only this process occurred, then a measurement of $M_z(\omega', t)$ at $\omega' = \omega$ would constitute a direct measurement of T_1. Furthermore a measurement of the hole width would yield a time-independent result, thereby determining δ. Hunklinger and Arnold have given such an interpretation to their experimental results, thereby obtaining $T_1 \approx 1$ μsec and
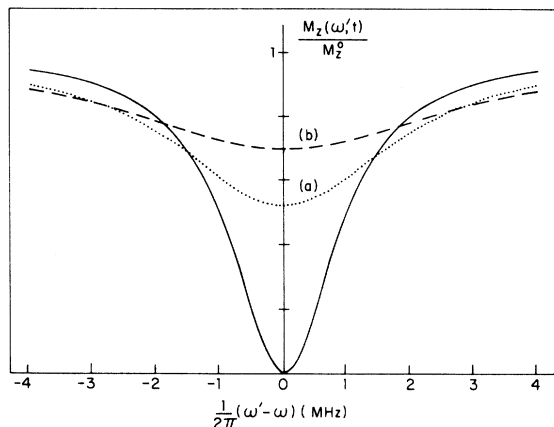

FIG. 11. Theoretical saturation recovery curves for $M_z(\omega', t)$ following a strong ultrasonic pulse at a frequency ω. The curves are derived from Eq. (33) with $\Delta\omega(t)$ taken from Fig. 4 at $T = 100$ mK. The "burned hole" of assumed width $\delta/2\pi = 1$ MHz at $t = 0$ is shown as the solid curve. The effect of spectral diffusion is shown by the dotted curve (a) at $t = 2$ μsec and by the dashed curve (b) at $t = 10$ μsec.

$\delta/2\pi \approx 50$ MHz with $T = 550$ mK and $\omega/2\pi = 0.74$ GHz.[4] They also observe that δ is proportional to T [cf. Eq. (20)] and ascribe this width to spin-spin interactions.

We wish to point out that spectral diffusion, as discussed in Sec. IV, is the correct description of the effects of spin-spin interactions upon saturation recovery experiments. The spectral diffusion kernel of Eq. (16) describes processes in which spins wander in and out of the hole, leading to the type of evolution indicated by curves (a) and (b) in Fig. 11. The hole becomes broader and shallower as time increases. This result[38] can be seen explicitly by convoluting Eqs. (16) and (32):

$$M_z(\omega', t) = \int d\omega'' D(\omega' - \omega'', t) M_z(\omega'', t = 0)$$

$$= M_z^0(\omega) \left(1 - \frac{\delta[\delta + \Delta\omega(t)]}{(\omega' - \omega)^2 + [\delta + \Delta\omega(t)]^2} \right). \qquad (33)$$

From this expression we see that the hole width increases in time as $\delta + \Delta\omega(t)$. On the other hand, the depth of the hole decreases with time as may be seen from (33) at the center of the hole ($\omega' = \omega$):

$$M_z(\omega, t) = M_z^0(\omega) \Delta\omega(t) / [\delta + \Delta\omega(t)] . \qquad (34)$$

The observability of the diffusion-induced time-dependent recovery effects summarized in Eqs. (33) and (34) depends upon several factors. Observation of time-dependent hole widths and hole depths requires that $\Delta\omega(t)$ be of the order of δ in a time interval where $\Delta\omega(t)$ shows significant time dependence. Furthermore the condition $t < T_1$ must hold to ensure that erasure of the hole due to direct A-spin relaxation does not occur. Finally for hole width experiments $\Delta\omega(t)$ must exceed the instrumental frequency resolution.

From Figs. 3–5 we can draw the following qualitative conclusions. At the lowest temperatures ($T = 20$ mK), $\Delta\omega(t)/2\pi < 0.2$ MHz for times less than T_1 (we estimate $T_1 \approx 160$ μsec for $\omega'/2\pi = 0.68$ GHz). Thus the time-dependent width and hole depth may be very difficult to observe at this temperature as a result of resolution problems. At the highest temperature ($T = 500$ mK), Fig. 5 shows that for $\eta = 10$, $\Delta\omega(t)/2\pi$ has the values 24 and 36 MHz at the times 1 and 10 μsec, respectively. At this temperature the A-spin T_1 for a 0.74-GHz phonon pulse is estimated to be 6 μsec. For times less than this value, a time-dependent hole width should be observable. As mentioned earlier, Hunklinger and Arnold report a width of 50 MHz at $T = 550$ mK, in rough agreement with our predictions. Unfortunately no attempt to measure the time dependence of the hole width was reported. Their measurement of hole depth led to a value of 1 μsec for T_1 at $T = 550$ mK and $\omega/2\pi = 0.74$ GHz. This T_1 is con-

siderably shorter than the value we predicted above. It is possible that this conflict may be resolved by including Eq. (34) to describe the recovery of the hole. Unfortunately, we are hampered by our lack of knowledge about δ. If we assume that $\delta = 150$ μsec^{-1}, we obtain $M_z(\omega, t)/M_z^0(\omega) = 0.5$ after 1 μsec when $\eta = 10$. Thus spectral diffusion provides a plausible explanation for the observed recovery. Finally for temperatures intermediate between 20 and 500 mK (cf. Fig. 4), the overall magnitude of $\Delta\omega(t, T)$ decreases from the high-temperature value, making measurements of hole width more difficult. On the other hand the larger value of the A-spin T_1 at this temperature (we estimate 39 μsec for $\omega'/2\pi = 0.68$ GHz) may make it easier to directly observe the time dependence of $\Delta\omega(t, T)$. In Fig. 11 we show the predictions deduced from Eq. (33) and Fig. 4 for recovery at $t = 2$ μsec and $t = 10$ μsec following saturation. For simplicity we have made the somewhat arbitrary choice, $\delta/2\pi = 1$ MHz. In a real experiment δ will depend on the spin packet width T_2^{-1} and on the saturating pulse power. Nevertheless it is quite conceivable that the time dependence of the recovering hole width, as shown in Fig. 11, will be observable near $T = 100$ mK.

VII. SUMMARY

The primary result of this paper is the confirmation of earlier work[4,12] which indicated that "spin-spin" interactions are essential to our understanding of the ultrasonic properties of glasses at low temperatures. The new feature which we have presented is spectral diffusion, which is derived from the time-dependent fluctuations of the local field seen by a spin (i.e., frequency modulation). We have argued, in fact, that such dynamic effects are the only observable consequences of spin-spin interactions in glasses. Using this concept of spectral diffusion, we have made predictions for phonon echo experiments and saturation experiments. The details of our predictions rely upon the "standard" tunneling level model of glasses, but we also note that our approach will apply to any type of excitation which couples to phonons.

By assuming that standard tunneling-level spins, parametrized by $(\overline{P}, \gamma_\alpha, \eta)$, are responsible for ultrasonic attenuation and echoes, we are able to place some restrictions on the parameters of these tunneling levels. The reasonable agreement between theory and experiment for two-pulse echo decay is support for the values of $\overline{P}$ and γ_α determined from unsaturated ultrasonic attenuation and echo pulse area measurements.[11,21] It must be noted, however, that our theory does not deter-

mine these parameters uniquely. The parameter η, which describes the extent of long relaxation times, has little effect on the ultrasonic experiments we have discussed. The short-time two-pulse echo decay envelopes are essentially independent of η (cf. Fig. 3) unless η is unreasonably small. The three-pulse experiments permit a probe of longer times, thus giving η a more visible effect (cf. Figs. 8 and 9). Nevertheless it seems unlikely that these experiments can ever extend to long enough times (because of A-spin T_1 processes) to distinguish between various reasonable values of η. Thus we should view the echo experiments as a way of verifying the spectral diffusion mechanism and of estimating $\overline{P}$ and γ_α. Predictions for saturation experiments have a similar importance. It is apparent that a direct measurement[4] of an A-spin T_1 [cf. Eq. (9)] by saturation recovery $[M_z(\omega, t)]$ would constitute a very straightforward way of determining the all-important coupling constants γ_α. Our discussion in Sec. VI, however, serves as a warning that measurements of $M_z(\omega, t)$ may be strongly affected by spectral diffusion so as not to be directly related to an A-spin T_1. The coupling constants γ_α do, of course, determine the rate at which spectral diffusion occurs (through T_1 for B spins). This means that any observation of a time-dependent hole depth or hole width provides indirect information on the coupling constants. In addition the observation of a time-dependent hole width would provide a striking confirmation of the existence of spectral diffusion in glasses.

In summary the spectral diffusion treatment of spin-spin interactions allows us to test the consistency among estimates of $\overline{P}$ and γ_α for standard tunneling levels. The experiments to which spectral diffusion applies generally do not involve long enough times to distinguish among values of η unless we allow η to be unreasonable small ($\eta \lesssim 3$). On the other hand, measurements of the specific heat of glasses do address the question of long relaxation times and could in principle be used to estimate η from Eqs. (10a) and (10b) using our knowledge of $\overline{P}$. Unfortunately we have seen in Sec. II that n_s, the standard-level density of states contributing to the specific heat, cannot be larger than $\frac{1}{2}\overline{P} \ln(4tR_{max})$ for any choice of η. Thus with the parameters we have used in this paper, it is impossible to account for the observed specific heat with "standard" levels alone. This situation has led us to introduce "anomalous" tunneling levels which affect the specific heat but not the ultrasonic properties. Preliminary considerations discussed in Sec. II suggest that even this scheme has difficulty in explaining the heat-pulse experiments of Gaubau and Tait.[18] We must bear

in mind, however, that to this date the crucial experiments[4,11,18,21] have been performed on different *types* of vitreous silica so that no rigorous comparisons can be made. Furthermore experimental uncertainties[4,11,21] in such quantities as $\bar{P}$ and γ_α are large enough (i.e., factors of 2) to allow for the possibility of reconciliation between theory and experiment. What we have seen in this paper is that one particular choice of parameters is not able to explain all experimental results. Detailed predictions for time-dependent specific-heat experiments in the presence of standard and anomalous levels with various choices of parameters will be presented in a separate publication.[39]

ACKNOWLEDGMENTS

APPENDIX

Here we derive the "spin-spin" coupling energy J_{ij}. We explicitly consider the tensor character of the coupling between spins and the elastic degrees of freedom. To this end we rewrite the relevant terms from Eq. (2) as

$$\mathcal{H}_1^{\text{elastic}} = - \sum_{i\alpha\beta} (B^i_{\alpha\beta}\epsilon^i_{\alpha\beta}S^i_x + D^i_{\alpha\beta}\epsilon^i_{\alpha\beta}S^i_z) , \tag{A1}$$

where $\epsilon^i_{\alpha\beta}$ is the strain tensor at site i, and

$$S_x = \frac{1}{2}\begin{pmatrix} 0 & 1 \\ 1 & 0 \end{pmatrix}, \quad S_y = \frac{1}{2}\begin{pmatrix} 0 & -i \\ i & 0 \end{pmatrix},$$

and $\tag{A1'}$

$$S_z = \frac{1}{2}\begin{pmatrix} 1 & 0 \\ 0 & -1 \end{pmatrix}.$$

Using Eq. (5) the tensors D and B are related to a tensor γ whose eigenvalues are assumed to be site independent:

$$D^i_{\alpha\beta} = 2\gamma_{\alpha\beta}\Delta^i/E^i , \tag{A2}$$
$$B^i_{\alpha\beta} = 2\gamma_{\alpha\beta}\Delta_0^i/E^i .$$

The eigenvalues of γ are determined by ultrasonic attenuation as in Eq. (8) and as in Eq. (A13).

A. Elastic-dipole strain field

The spins of Eq. (A1) are considered to be embedded in an isotropic elastic continuum described by longitudinal and transverse sound velocities c_l and c_t. The strain tensor is related to the displacement vector u_α by (see, for example, Ref. 40)

$$\epsilon_{\alpha\beta} = \tfrac{1}{2}(\partial_\alpha u_\beta + \partial_\beta u_\alpha) . \tag{A3}$$

The term $D^j_{\alpha\beta}S^j_z$ in Eq. (A1) represents an external stress localized at site j. By requiring that this external stress be balanced by internal stress in the elastic continuum, we obtain[10] (taking site j to be the origin and suppressing the superscript j)

$$\rho c_t^2 \nabla^2 u_\alpha + \rho(c_l^2 - c_t^2)\partial_\alpha(\partial_\nu u_\nu) = (D_{\alpha\beta}S_z)\partial_\beta\delta(\vec{r}) . \tag{A4}$$

In deriving (A4) we have used (A3) and Hooke's law. Equation (A4) may now be solved to yield the displacement field at $\vec{r}$ resulting from a single elastic dipole at the origin:

$$u_\alpha(\vec{r}) = \frac{S_z}{8\pi\rho}\left[\left(\frac{1}{c_t^2} - \frac{1}{c_l^2}\right)\left(\frac{r_\alpha D_{\nu\nu}}{r^3} - 3\frac{r_\alpha r_\beta r_\nu D_{\beta\nu}}{r^5}\right) - \frac{2}{c_l^2}\frac{D_{\alpha\beta}r_\beta}{r^3}\right]. \tag{A5}$$

The strain field at $\vec{r}$ is then obtained with the use of Eq. (A3):

$$\epsilon_{\alpha\beta}(\vec{r}) = -S_z(\Delta/E)(1/r^3) T_{\alpha\beta}(\hat{r}) ,$$

where

$$T_{\alpha\beta}(\hat{r}) = \frac{1}{4\pi\rho}\left\{\frac{2\gamma_{\alpha\beta}}{c_l^2} + 3\left(\frac{1}{c_t^2} - \frac{2}{c_l^2}\right)\right.$$
$$\times \left(\frac{r_\alpha r_\nu \gamma_{\beta\nu} + r_\beta r_\nu \gamma_{\alpha\nu}}{r^2}\right)$$
$$+ \left(\frac{1}{c_t^2} - \frac{1}{c_l^2}\right)\left[\left(-\delta_{\alpha\beta} + \frac{3r_\alpha r_\beta}{r^2}\right)\gamma_{\nu\nu}\right.$$
$$\left.\left. + 3\left(\delta_{\alpha\beta} - \frac{5r_\alpha r_\beta}{r^2}\right)\frac{r_\nu r_\mu \gamma_{\nu\mu}}{r^2}\right]\right\}, \tag{A6}$$

and we imply summation over repeated indices. In the case of purely isotropic coupling ($\gamma_{\alpha\beta} = \gamma\delta_{\alpha\beta}$), Eq. (A6) reduces to an expression reminiscent of the familiar electric-dipole field:

$$\epsilon_{\alpha\beta}(\vec{r}) = \frac{-2\gamma(\Delta/E)S_z}{4\pi\rho c_l^2 r^3}\left(\delta_{\alpha\beta} - \frac{3r_\alpha r_\beta}{r^2}\right). \tag{A7}$$

In general, however, we cannot assume that $\gamma_{\alpha\beta}$ has the simple form which leads Eq. (A7). Instead we employ Eq. (A6) and use the fact that the symmetric tensor $\gamma_{\alpha\beta}$ is uniquely determined by its three eigenvalues and its mutually orthogonal eigenvectors (see, for example, Ref. 17).

B. Interaction energy and angular averaging

It is now straightforward to obtain the interaction energy J_{ij} of Eqs. (11) and (12). The internal strain at site i arising from a spin at site j is given by Eq. (A6) with $S_z = S^j_z$, $\gamma_{\alpha\beta} = \gamma^j_{\alpha\beta}$, $\vec{r} = \vec{r}_{ij}$, and $T_{\alpha\beta} = T^j_{\alpha\beta}$. This strain is then substituted for $\epsilon^i_{\alpha\beta}$ in the second term of Eq. (A1), yielding an interaction as in Eq. (12) with

$$J_{ij} = \sum_{\alpha\beta} \left(2\frac{\Delta^i}{E^i}\gamma^i_{\alpha\beta} \right)\left(\frac{\Delta^j}{E^j}\frac{1}{r^3_{ij}} T^j_{\alpha\beta}(\hat{r}_{ij}) \right)$$

$$= C_{ij}\frac{\Delta^i}{E^i}\frac{\Delta^j}{E^j}\frac{1}{r^3_{ij}} , \tag{A8}$$

where

$$C_{ij} \equiv 2\gamma^i_{\alpha\beta}T^j_{\alpha\beta}(\hat{r}_{ij}) \tag{A8'}$$

In these expressions, we have employed Eq. (A2) in order to explicitly display the factors in J_{ij} which depend upon the tunneling model parameter Δ/E. We have verified that Eq. (A8) agrees with the results of Joffrin and Levelut[12] in the special cases they considered. For example, in the case of isotropic coupling as in Eq. (A7), we obtain

$$J_{ij} = \sum_{\alpha\beta} 2\gamma^i\frac{\Delta^i}{E^i} \delta_{\alpha\beta}\frac{2\gamma\Delta^j/E^j}{4\pi\rho c_l^2 r^3_{ij}} \left(\delta_{\alpha\beta} - \frac{3r_\alpha r_\beta}{r^2} \right) = 0 \tag{A9}$$

in agreement with their results.

In order to estimate the magnitude of J_{ij} we must take into account its complicated dependence upon $\gamma^i_{\alpha\beta}$, $\gamma^j_{\alpha\beta}$, and $\hat{r}_{ij}$ as expressed in Eq. (A8). As mentioned above, the tensors $\gamma^i_{\alpha\beta}$ and $\gamma^j_{\alpha\beta}$ are each described by the orientation of their eigenvectors. We can always choose a reference frame whose axes coincide with the eigenvectors at site i. We must then average over the three Euler angles which determine the orientation of the eigenvectors at site j in this reference frame. We must also average over the orientation of $\hat{r}_{ij}$ in this reference frame. A straightforward but tedious calculation yields

$$C^2_{\text{rms}} \equiv \langle C^2_{ij}\rangle$$

$$= \frac{2}{75}\left(\frac{1}{2\pi\rho}\right)^2 \left\{ \left[(13A_1 + A_2)^2 - 4(37A_1^2 + 3A_2^2) \right] c_l^{-4} \right.$$

$$\left. + (3A_1 - A_2)^2(c_t^{-2} - c_l^{-2})(9c_t^{-2} - 7c_l^{-2}) \right\}, \tag{A10}$$

where $A_1 \equiv \text{Tr}\gamma^2$ and $A_2 \equiv (\text{Tr}\gamma)^2$. The constants A_1, A_2 are related to the measurable coupling constants γ_l^2, γ_t^2, as is shown in Eq. (A13). It is a simple matter to check that $C_{\text{rms}} = 0$ (as it should) for the case of isotropic coupling, in which $A_2 = 3A_1$.

It is important to notice that C_{rms} is an upper bound for the quantity $\langle|C_{ij}|\rangle$ since

$$\langle [|C_{ij}| - \langle|C_{ij}|\rangle]^2\rangle = \langle C^2_{ij}\rangle - \langle|C_{ij}|\rangle^2 \geq 0 . \tag{A11}$$

It is the quantity $\langle|C_{ij}|\rangle$ which appears in the exact expression for the spectral diffusion width in the case of $1/r^3$ interactions.[13,24] Unfortunately the calculation of $\langle|C_{ij}|\rangle$ is not feasible because of the difficulty in keeping track of the sign changes in Eq. (A8).

It is very difficult to determine exactly how good C_{rms} is as an upper bound to $\langle|C_{ij}|\rangle$. One simple case in which we can compare results is the "semi-isotropic" case. Here we assume that $\gamma^j_{\alpha\beta} = \gamma^j\delta_{\alpha\beta}$ so that Eq. (A7) replaces Eq. (A6). If we also assume that $\gamma^i_{\alpha\beta} = \gamma^i\delta_{\alpha\beta}$, we get the trivial result of Eq. (A9). Instead we assume that the coupling at site i is anisotropic. In particular we assume that site i is described by $A_1 = A_2 = \gamma^i$, corresponding to one nonzero eigenvalue γ^i, and two zero eigenvalues of $\gamma^i_{\alpha\beta}$. In this simple case we find

$$C_{\text{rms}} = 0.89|2\gamma^j| \, |2\gamma^i|/4\pi\rho c_l^2 ,$$

$$\langle|C_{ij}|\rangle = 0.77|2\gamma^j| \, |2\gamma^i|/4\pi\rho c_l^2 . \tag{A12}$$

Taking the ratio, we find $\langle|C_{ij}|\rangle/C_{\text{rms}} = 0.87$.

C. Calculating C_{rms} from coupling constants

In order to determine C_{rms}, it is necessary to have values for A_1 and A_2. These two coupling constants are uniquely determined by the coupling constants γ_l and γ_t which appear in Eq. (8). Our task now is to relate these two sets of parameters. This calculation has already been performed elsewhere,[17] and involves averaging over the relative orientations of $\gamma_{\alpha\beta}$ and the phonon propagation vector. The results are

$$\gamma_l^2 = \tfrac{1}{15}(2A_1 + A_2) , \quad \gamma_t^2 = \tfrac{1}{30}(3A_1 - A_2) . \tag{A13}$$

Substituting into Eq. (A10), we obtain

$$C_{\text{rms}} = (\sqrt{6}/\pi\rho)[\gamma_t^2(4\gamma_l^2 - 3\gamma_t^2)c_l^{-4}$$

$$+ \gamma_t^4(c_t^{-2} - c_l^{-2})(9c_t^{-2} - 7c_l^{-2})] . \tag{A14}$$

Measurements of pulse areas in echo experiments[11] suggest a value of 1.6 eV for γ_l. Furthermore the relation $\gamma_t^2 \approx \tfrac{1}{2}\gamma_l^2$ is suggested by measurements of both transverse and longitudinal ultrasonic attenuation.[21] Thus we obtain

$$C_{\text{rms}} = 1.6 \times 10^{-35} \text{ erg cm}^3 , \tag{A15}$$

by using the values $c_l = 5.8 \times 10^5$ cm/sec, $c_t = 3.8 \times 10^5$ cm/sec and $\rho = 2.2$ g/cm^3, which are appropriate for vitreous silica.[4]

[1]R. O. Pohl and G. L. Salinger, Ann. N. Y. Acad. Sci. <u>279</u>, 150 (1976).

[2] R. C. Zeller and R. O. Pohl, Phys. Rev. B $\underline{4}$, 2029 (1971).

[3] R. B. Stephens, Phys. Rev. B $\underline{8}$, 2896 (1973).

[4] S. Hunklinger and W. Arnold, in *Physical Acoustics*, edited by R. N. Thurston and W. P. Mason (Academic, New York, 1976), Vol. 12, p. 155; W. Arnold and S. Hunklinger, Solid State Commun. $\underline{17}$, 883 (1975).

[5] B. Golding, J. E. Graebner, B. I. Halperin, and R. J. Schutz, Phys. Rev. Lett. $\underline{30}$, 223 (1973).

[6] W. Arnold, S. Hunklinger, S. Stein, and K. Dransfeld, J. Non-Cryst. Solids $\underline{14}$, 192 (1974); J. Jäckle, L. Piché, W. Arnold, and S. Hunklinger, *ibid.* $\underline{20}$, 365 (1976).

[7] L. Piché, R. Maynard, S. Hunklinger, and J. Jäckle, Phys. Rev. Lett. $\underline{32}$, 1426 (1974).

[8] B. Golding, J. E. Graebner, and A. B. Kane, Phys. Rev. Lett. $\underline{37}$, 1248 (1976).

[9] M. von Schickfus and S. Hunklinger, J. Phys. C $\underline{9}$, L439 (1976).

[10] P. Doussineau, A. Levelut, and T. A. Thu-Thuy, J. Phys. Lett. (Paris) $\underline{38}$, L37 (1977).

[11] B. Golding and J. E. Graebner, Phys. Rev. Lett. $\underline{37}$, 852 (1976).

[12] J. Joffrin and A. Levelut, J. Phys. (Paris) $\underline{36}$, 811 (1976).

[13] J. R. Klauder and P. W. Anderson, Phys. Rev. $\underline{125}$, 912 (1962).

[14] P. W. Anderson, B. I. Halperin, and C. M. Varma, Philos. Mag. $\underline{25}$, 1 (1972).

[15] W. A. Phillips, J. Low-Temp. Phys. $\underline{7}$, 351 (1972).

[16] J. Jäckle, Z. Phys. $\underline{257}$, 212 (1972).

[17] B. I. Halperin, Ann. N. Y. Acad. Sci. $\underline{279}$, 173 (1976).

[18] S. Hunklinger, P. Piché, J. C. Lasjaunias, and K. Dransfeld, J. Phys. C $\underline{8}$, L423 (1975).

[19] R. B. Stephens, Phys. Rev. B $\underline{13}$, 852 (1975).

[20] W. M. Goubau and R. H. Tait, Phys. Rev. Lett. $\underline{34}$, 1220 (1975).

[21] B. Golding, J. E. Graebner, and R. J. Schutz, Phys. Rev. B $\underline{14}$, 1660 (1976).

[22] J. C. Lasjaunias, R. Ravex, M. Vandorpe, and S. Hunklinger, Solid State Commun. $\underline{17}$, 1045 (1975).

[23] In particular, most of the spins experience a random static "magnetic field" which is much larger than the interaction between spins. This rules out the possibility of a phase transition or of a hole in the density of states near zero frequency, such as has been predicted for the so-called spin glass state of magnets with random interactions. See, for example, D. J. Thouless, P. W. Anderson, and R. G. Palmer, Philos. Mag. $\underline{35}$, 593 (1977).

[24] W. B. Mims, in *Electron Paramagnetic Resonance*, edited by S. Geschwind (Plenum, New York-London, 1972).

[25] Averages of quantities over the ensemble of A spins (spins resonant with an ultrasonic pulse) must be weighted in favor of those spins which have a strong off-diagonal coupling to phonons. Since this coupling is proportional to Δ_0^2/E^2 [cf. Eq. (5)], we define the weighted average of any quantity F as $\langle F \rangle_A \equiv \langle \Delta_0^2 F \rangle_\lambda / \langle \Delta_0^2 \rangle_\lambda$. For example, using this prescription, we obtain $\langle |\Delta/E| \rangle_A = \frac{1}{2}$.

[26] A. Abragam, *The Principles of Nuclear Magnetism* (Clarendon, Oxford, 1961).

[27] I. D. Abella, N. A. Kurnit, and S. R. Hartmann, Phys. Rev. $\underline{141}$, 391 (1966).

[28] P. Hu and S. R. Hartmann, Phys. Rev. B $\underline{9}$, 1 (1974).

[29] G. M. Zhidomirov and K. M. Salikhov, Sov. Phys.-JETP $\underline{29}$, 1037 (1969).

[30] B. Golding and J. E. Graebner (unpublished).

[31] W. B. Mims, Phys. Rev. $\underline{168}$, 370 (1968).

[32] S. L. McCall and E. L. Hahn, Phys. Rev. $\underline{183}$, 457 (1969).

[33] A. M. Portis, Phys. Rev. $\underline{91}$, 1071 (1953).

[34] N. Bloembergen, S. Shapiro, P. S. Pershan, and J. O. Artman, Phys. Rev. $\underline{114}$, 445 (1959).

[35] A. M. Portis, Phys. Rev. $\underline{104}$, 584 (1956).

[36] E. L. Wolf, Phys. Rev. $\underline{142}$, 555 (1966).

[37] G. Feher, Phys. Rev. $\underline{114}$, 1219 (1959).

[38] W. B. Mims, K. Nassau, and J. D. McGee, Phys. Rev. $\underline{123}$, 2059 (1961).

[39] J. L. Black (unpublished).

[40] For this equation with a different type of source term, see Eqs. 7.2, 22.2, and 22.6 in L. D. Landau and E. M. Lifshitz, *Theory of Elasticity*, 2nd English ed. (Pergamon, New York, 1970).